PHYSICAL REVIEW A VOLUME 57, NUMBER 2 FEBRUARY 1998

Resonant coherent excitation of surface channeled ions

K. Kimura* and M. Mannami
Department of Engineering Physics and Mechanics, Kyoto University, Kyoto 606-01, Japan

(Received 2 September 1997)

The resonant coherent excitation (RCE) of surface channeled ions has been theoretically investigated. Solving the Schrödinger equation numerically along the ion trajectory, the excitation probability of the surface channeled ion due to the periodic components of the surface potential is calculated. The mixing and energy shift of the electronic states in the vicinity of the surface due to both the continuum surface potential and the induced surface wake potential are included. The result is compared with the recent experimental result of the RCE of surface channeled B^{4+} ions at a SnTe(001) surface. Using a *freezing distance* model for the charge exchange processes, the characteristic features of the observed result can be well reproduced. This indicates that the observed RCE occurs mainly in the outgoing trajectory. [S1050-2947(98)04002-5]

PACS number(s): 79.20.Rf, 34.50.Fa, 61.85.+p

I. INTRODUCTION

When an ion passes through an axial channel in a single crystal, the channeled ion experiences sequential collisions with crystal atoms. These collisions cause a periodic perturbation of frequency $\nu = v/d$, where v is the ion velocity and d is the atomic spacing along the atomic string. If the excitation energy of the ion, ΔE, coincides with the frequency or one of its higher harmonics,

$$\Delta E = 2\pi\hbar \frac{kv}{d}, \tag{1}$$

the excitation may occur, where k is an integer. This phenomenon, called resonant coherent excitation (RCE), was predicted by Okorokov [1] and a successful measurement was done by Datz *et al.* [2]. They observed the reduction of the incident charge state fraction after passing through thin crystal foils at the resonance energy. The observed reduction was attributed to the large electron loss probability of the excited ions created by RCE. From the detailed observation of the resonance profile, the energy shift and splitting of the excited states due to the polarization wake in a crystal channel were clearly demonstrated [2,3]. In addition to the observation of RCE through the change in the charge state distribution, recent investigations have shown enhancements of projectile x-ray emission [4,5] and of convoy electron emission [6] under resonance conditions.

Just after the observation of RCE, Kupfer, Gabriel, and Burgdörfer discussed RCE of surface channeled ions [7]. Although several theoretical studies revealed characteristic features of the surface RCE [8–11], it has been believed that there is an intrinsic difficulty in the observation of the surface RCE [8,12]. In order to observe a sharp resonance, the ion has to travel along the atomic string for a long distance. This can be realized at a small angle of incidence as can be seen in Fig. 1, where trajectories of surface channeled ions are shown for various incident angles. Decreasing incident angle, however, the distance of the closest approach to the surface becomes larger. Because the periodic perturbation decreases very rapidly with distance from the surface, the small incident angle results in a small RCE probability.

Recently, the RCE of surface channeled ions was first observed through the change of the charge state distribution of surface channeled ions [13]. The observed change was very weak as expected by the above discussion. It was, however, suggested that the observed weak effect might be attributed to the large charge exchange probability in the vicinity of the surface [13]. In the present paper, the RCE of surface channeled ions is theoretically investigated. The calculated RCE probability is compared with the experimental result in order to see whether the weak effect is due to the intrinsic difficulty. The effect of the charge exchange process on the surface RCE is discussed using a freezing distance model.

II. EXPERIMENTAL RESULT

The details of the experimental result were described elsewhere [13,14]; here only the relevant result is given. A beam of B^{3+} ions from a Tandetron accelerator was collimated by

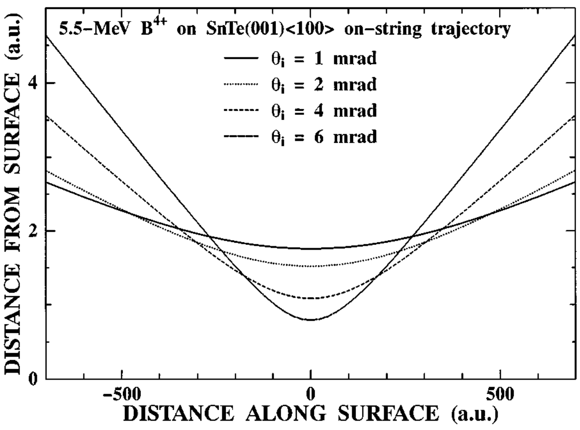

FIG. 1. Trajectories of surface channeled 5.5-MeV B^{4+} ions on a SnTe(001) surface at various incident angles.

---

*Author to whom correspondence should be addressed. Fax number: +81-75-753-5253. Electronic address: kimura@kues.kyoto-u.ac.jp.

1050-2947/98/57(2)/1121(5)/$15.00

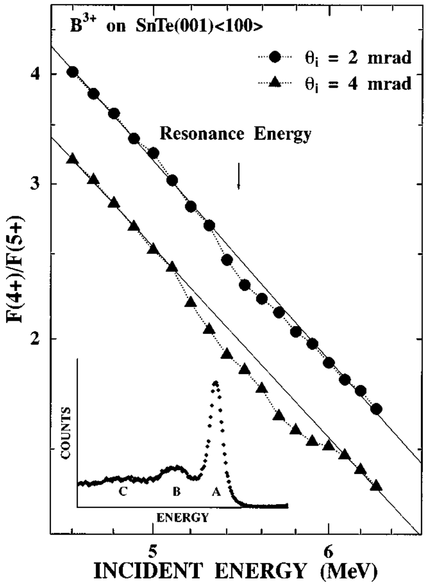

FIG. 2. Ratio of the B^{4+} fraction to the B^{5+} fraction observed at the specular angle when B^{3+} ions are incident on a SnTe(001) surface along the [100] axis at $\theta_i = 2$ and 4 mrad. The lines are drawn to guide the eye. The statistical error is smaller than the symbols. The inset shows an example of the observed energy spectrum of the surface channeled ions.

a series of apertures to less than $0.1 \times 0.1\ \mathrm{mm}^2$ and to a divergence angle less than 0.3 mrad. The beam was incident on the SnTe(001) surface at glancing angles 2–6 mrad under [100] surface channeling condition. The ions scattered at a specular angle were energy analyzed by a 90° sector magnetic spectrometer. An example of the observed energy spectrum is shown in the inset of Fig. 2. The energy spectrum shows several well defined peaks which are related to particular ion trajectories. The most pronounced peak labeled *A* was found to correspond to an on-string trajectory [13,15]. The charge state distribution of the ions of this peak was measured at the incident energies 4.6–6.3 MeV. The B^{4+} fraction was dominant (>50%) and the B^{3+} fraction was small in the present energy region, showing that the incident B^{3+} ions were efficiently ionized in the vicinity of the surface. Although we studied the RCE of B^{4+} ions, this fact allowed us to use the B^{3+} beam as an incident beam. The observed ratio of the B^{4+} fraction to the B^{5+} fraction, $F(4+)/F(5+)$, is shown in Fig. 2. There is a small reduction of B^{4+} fraction around 5.5 MeV. This energy agrees with the resonance energy (5.46 MeV) of the B^{4+} ion from $n=1$ to $n=2$ states for $k=2$, showing that the observed B^{4+} reduction is caused by the RCE.

III. CALCULATION AND DISCUSSION

An electron bound to a surface channeled ion is affected by a periodic potential

$$V(\mathbf{r}) = \sum_k V_k(y,z) e^{-ik(2\pi/d)x}, \tag{2}$$

where the x axis is parallel to the string, the z axis is perpendicular to the surface, and $V_k(y,z)$ can be written as

$$V_k(y,z) = \frac{1}{d} \int_{-\infty}^{+\infty} V_{\mathrm{atom}}(\mathbf{r}) e^{ik(2\pi/d)x} dx, \tag{3}$$

where the single string model is employed and $V_{\mathrm{atom}}(\mathbf{r})$ is the atomic potential. The electron is also affected by an image potential $V_{\mathrm{img}}(\mathbf{R}_{\mathrm{ion}},\mathbf{r})$, which is induced by the ion located at $\mathbf{R}_{\mathrm{ion}}[=(X_{\mathrm{ion}},Y_{\mathrm{ion}},Z_{\mathrm{ion}})]$ near the surface. We will focus on a surface channeled hydrogenlike ion of atomic number Z_1 traveling along the on-string trajectory. In the calculation of $V_{\mathrm{img}}(\mathbf{R}_{\mathrm{ion}},\mathbf{r})$, the hydrogenlike ion is approximated by a point charge of $(Z_1-1)e$. In the projectile frame, the total Hamiltonian for the electron is written as

$$H = -\frac{\hbar^2}{2m}\Delta_{r_e} - \frac{Z_1 e^2}{r_e} + U(\mathbf{R}_{\mathrm{ion}}(t),\mathbf{r}_e) + W(\mathbf{R}_{\mathrm{ion}}(t),\mathbf{r}_e), \tag{4}$$

where

$$U(\mathbf{R}_{\mathrm{ion}}(t),\mathbf{r}_e) = V_{\mathrm{img}}(\mathbf{R}_{\mathrm{ion}}(t),\mathbf{R}_{\mathrm{ion}}(t)+\mathbf{r}_e) + V_0(Y_{\mathrm{ion}}(t)+y_e, Z_{\mathrm{ion}}(t)+z_e), \tag{5}$$

$$W(\mathbf{R}_{\mathrm{ion}}(t),\mathbf{r}_e) = \sum_{k\neq 0} V_k(Y_{\mathrm{ion}}(t)+y_e, Z_{\mathrm{ion}}(t)+z_e) \times e^{-ik(2\pi/d)[X_{\mathrm{ion}}(t)+x_e]}, \tag{6}$$

and $\mathbf{r}_e[=(x_e,y_e,z_e)]$ is the position of the electron with respect to the nucleus of the ion. While $U(\mathbf{R}_{\mathrm{ion}}(t),\mathbf{r}_e)$ changes slowly along the trajectory, $W(\mathbf{R}_{\mathrm{ion}}(t),\mathbf{r}_e)$ oscillates rapidly with a frequency about $k\nu/d$. Thus the former causes adiabatic change of the bound state and the latter is responsible to RCE. Note that the oscillatory term decreases very rapidly with increasing distance from the surface. This suggests that RCE occurs mainly around the closest approach of the ion trajectory.

In the first step, the adiabatic change of the electronic state of the surface channeled ion along the ion trajectory is calculated. The Schrödinger equation without the oscillatory term,

$$\left(-\frac{\hbar^2}{2m}\Delta_{r_e} - \frac{Z_1 e^2}{\mathbf{r}_e} + U(\mathbf{R}_{\mathrm{ion}},\mathbf{r}_e) \right) \psi_\alpha(\mathbf{R}_{\mathrm{ion}},\mathbf{r}_e) = E_\alpha(\mathbf{R}_{\mathrm{ion}}) \psi_\alpha(\mathbf{R}_{\mathrm{ion}},\mathbf{r}_e), \tag{7}$$

is solved using the first-order perturbation theory. This procedure is the same as the calculation of the energy levels of hydrogenlike ions in a crystal channel inside a crystal except for the image potential in $U(\mathbf{R}_{\mathrm{ion}},\mathbf{r}_e)$ [16]. Figure 3 displays the calculated excitation energy of the 5.5-MeV B^{4+} ion from $n=1$ to $n=2$ states as a function of the distance from the surface. The $n=2$ states are split into four states, $(2s \pm 2p_z)$-like, $2p_x$-like, and $2p_y$ states due to $U(\mathbf{R}_{\mathrm{ion}},\mathbf{r}_e)$. In the calculation, the image potential given by Ohtsuki [17] was employed. The results calculated without the image potential are also shown by dotted curves. The good agreement between these curves (with and without the image potential) indicates that the effect of the image potential on the energy shift is negligibly small. Approaching the surface, the exci-

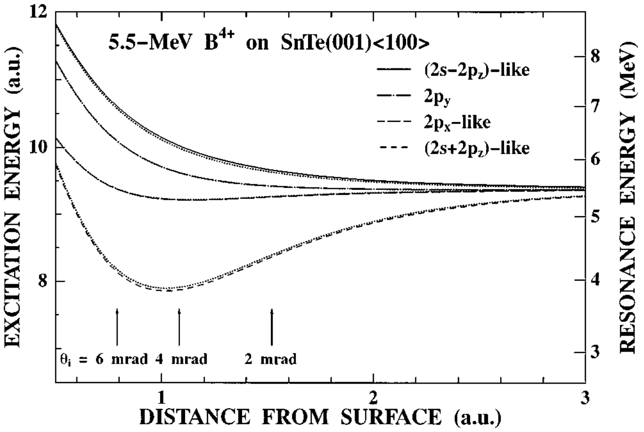

FIG. 3. Calculated excitation energies from $n=1$ to $n=2$ states for a channeled 5.5-MeV B^{4+} ion in the on-string trajectory at the SnTe(001) surface. The $2s$ mixes with $2p_x$ and $2p_z$ to make $(2s\pm 2p_z)$-like and $2p_x$-like substrates. The ordinate of the right-hand side shows the corresponding resonance energy for $k=2$ resonance. Arrows show the closest approaches for the surface channeled ions at $\theta_i=2$, 4, and 6 mrad.

tation energy and so the resonance energy changes. The ordinate in the right-hand side shows the resonance energy for $k=2$.

In the next step, the time-dependent Schrödinger equation including the oscillatory term, $W(\mathbf{R}_{\rm ion}(t),\mathbf{r}_e)$, is solved in order to estimate the RCE probability of the surface channeled ion. The electron wave function can be expressed in terms of the adiabatic wave functions,

$$\Psi(\mathbf{r}_e,t)=\sum_{\alpha=1}^{5} a_\alpha(t)\psi_\alpha(\mathbf{R}_{\rm ion}(t),\mathbf{r}_e)e^{-i[E_\alpha(\mathbf{R}_{\rm ion}(t))/\hbar]t}, \qquad (8)$$

where α denotes $n=1$ and 2 states. We consider only these states because we are considering the RCE from $n=1$ to $n=2$ states. Substituting Eq. (8) into the time-dependent Schrödinger equation, the differential equation for $a_\alpha(t)$ is obtained,

$$\begin{aligned}\dot{a}_\alpha(t)=&\frac{i}{\hbar}\,a_\alpha(t)\,\frac{d}{dt}\,[E_\alpha(\mathbf{R}_{\rm ion}(t))]t\\ &-\sum_\beta\left[\int \psi_\alpha(\mathbf{R}_{\rm ion}(t),\mathbf{r}_e)\,\frac{d\psi_\beta(\mathbf{R}_{\rm ion}(t),\mathbf{r}_e)}{dt}\,d\mathbf{r}_e\right.\\ &\left.+\frac{i}{\hbar}\,\langle\alpha|W(\mathbf{R}_{\rm ion}(t),\mathbf{r}_e)|\beta\rangle\right]a_\beta(t)\\ &\times e^{i\{[E_\alpha(\mathbf{R}_{\rm ion}(t))-E_\beta(\mathbf{R}_{\rm ion}(t))]/\hbar\}t}. \qquad (9)\end{aligned}$$

Employing an approximation,

$$W(\mathbf{R}_{\rm ion},\mathbf{r}_e)\simeq W(\mathbf{R}_{\rm ion},\mathbf{0})+\mathbf{r}_e\left.\frac{\partial W(\mathbf{R}_{\rm ion},\mathbf{r}_e)}{\partial r_e}\right|_{\mathbf{r}_e=\mathbf{0}}, \qquad (10)$$

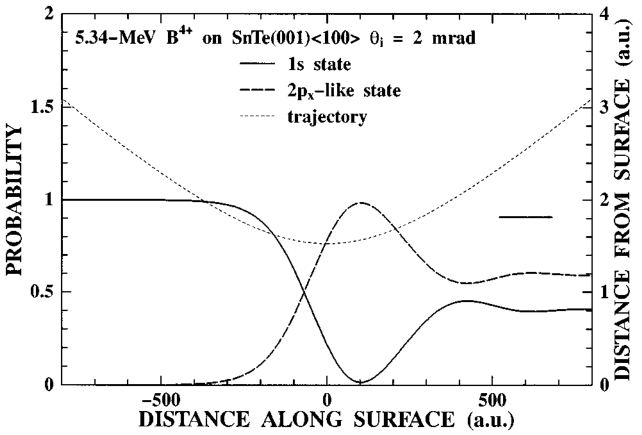

FIG. 4. Displayed is the evolution of the probabilities of occupancy of $n=1$ and 2 states along the ion trajectory when a 5.34-MeV B^{4+} ion is incident on a SnTe(001) surface along the [100] axis at $\theta_i=2$ mrad. The $2p_x$-like state is mainly excited around the closest approach. The short-dashed curve shows the ion trajectory.

Eq. (9) was solved numerically. The $2p_y$ state cannot be excited in the on-string trajectory because the oscillatory field does not have a y component. An example of the calculated result is shown in Fig. 4. The probabilities of occupancy of $n=1$ and 2 states of a surface channeled B^{4+} ion are shown along the on-string trajectory together with the ion trajectory when a 5.34-MeV B^{4+} ion in the ground state is incident at $\theta_i=2$ mrad. The probability of the $2p_x$-like state increases rapidly along the trajectory and the excitation probability of about 60% is obtained after reflection from the surface while other substates are hardly excited. This state-selective excitation can be understood by the following: The RCE mainly occurs around the closest approach, where the oscillatory term has a large value and the ion travels almost parallel to the surface. In the present case, the ion energy (5.34 MeV) coincides with the resonance energy from $1s$ to the $2p_x$-like state at the closest approach (1.5 a.u.), as can be seen from Fig. 3. Thus the $2p_x$-like state is mainly excited. It should be noted that the occupation probability of the $2p_x$-like state reaches almost 100% around the closest approach, and the probability decreases after this point (resonant coherent deexcitation).

Figure 5 displays the calculated RCE probability of the

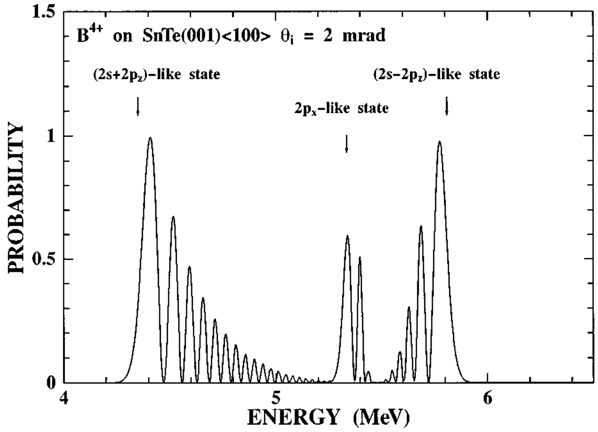

FIG. 5. Calculated RCE probability $(n=1\rightarrow n=2)$ of the surface channeled B^{4+} ion at $\theta_i=2$ mrad as a function of the ion energy. Arrows indicate the calculated resonance energies at the closest approach of the surface channeled ion at $\theta_i=2$ mrad.

surface channeled B^{4+} ion at $\theta_i = 2$ mrad as a function of the ion energy. The probability shows oscillatory structure. These oscillations are similar to the oscillations observed in the case of the potential-curve crossing. Aside from the oscillations, the RCE probability has a large value around ~4.4, ~5.3, and ~5.8 MeV. These energies are in agreement with the calculated resonance energies for the $(2s+2p_z)$-like, $2p_x$-like, and $(2s_s-2p_z)$-like states, respectively. The calculated large RCE probability clearly indicates that there is no intrinsic difficulty to observe the surface RCE. However, the observed RCE was very small, as is seen in Fig. 2. In addition, the calculated resonance profile extends from 4.2 to 6 MeV, while the RCE was observed in the energy region from 5.3 to 5.8 MeV. These disagreements might be attributed to the charge exchange processes near the surface which were neglected in the calculation. The B^{5+} ion created by the prompt ionization of the excited B^{4+} ion produced by RCE may capture an electron near the surface. Thus the effect of surface RCE on the charge state distribution might be erased by the subsequent charge exchange processes near the surface.

In a recent study, we demonstrated that 2-MeV C^{q+} ions have large charge exchange probabilities in the vicinity of the SnTe(001) surface [18]. A simple model called the freezing distance model was introduced to explain the charge state dependence of the observed energy losses of the carbon ions specularly reflected from the SnTe(001). In the model, the surface region is divided into two regions by a so-called freezing distance D_F. At $z<D_F$, the charge exchange probabilities are so large that an equilibrium charge state distribution is attained within a short distance. On the contrary, at $z>D_F$, the ion does not change its charge state. This simple model explained the observed energy losses very well and the freezing distance was determined to be about 3 a.u. [18]. Applying the freezing distance model to the present case, the reduction of the B^{4+} fraction caused by RCE is erased at $z<D_F$. Only the RCE occurring at $z>D_F$ in the outgoing trajectory can be observed.

Based on the freezing distance model, the probability of RCE, which occurs at $z>D_F$ in the outgoing trajectory, can be estimated from the observed result. The B^{4+} fraction, $F_0(4+)$, without RCE was estimated by the general trend of the energy dependence of the observed ratio, which is shown by a solid line in Fig. 2. Assuming that the excited B^{4+} ion loses its bound electron even at $z>D_F$, the RCE probability can be estimated by $\{F_0(4+)-F(4+)\}/F_0(4+)$. Figure 6 displays the RCE probability estimated from the observed result. The ion energy shown in Fig. 6 is the exit energy which is smaller than the incident energy by about 100 keV due to the energy loss. The estimated RCE probability is 2–3 % for incident angles 2–6 mrad. These results can be compared with the probability calculated by solving Eq. (9) after $z=D_F$ in the outgoing trajectory. The RCE probabilities calculated with various D_F are shown in Fig. 7 together with the experimental result. The calculated RCE probability shows three peaks corresponding to the excitations to the $(2s+2p_z)$-like, $2p_x$-like, and $(2s-2p_z)$-like states. The RCE probability decreases rapidly and the outer peaks shift towards the center with increasing D_F. These can be understood by the fact that the RCE occurs mainly just after $z=D_F$ in the outgoing trajectory because the periodic perturbation decreases very rapidly with z. The decrease of the RCE probability is a simple reflection of the rapid decrease of the periodic perturbation. The shift can be explained by the z-dependence of the Stark shift (see Fig. 3). The calculated result with $D_F \approx 2$ $a.u.$ agrees reasonably well with the experimental one except for the calculated peak around 5 MeV [which corresponds to the excitation to the $(2s+2p_z)$-like state], which does not appear in the experimental result. This might be attributed to the short lifetime of the $(2s+2p_z)$-like state in the vicinity of the surface. The

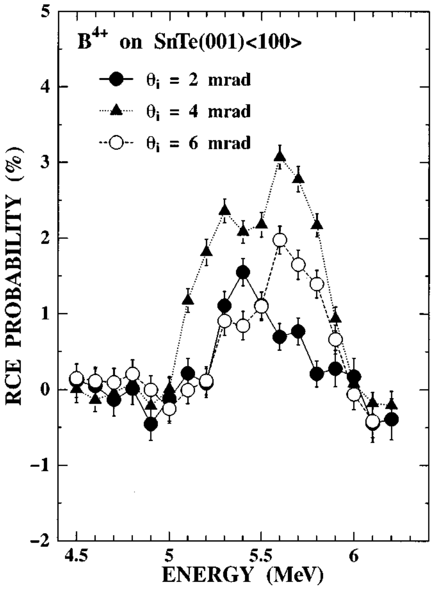

FIG. 6. RCE probability of the surface channeled B^{4+} ion estimated from the observed charge state distribution.

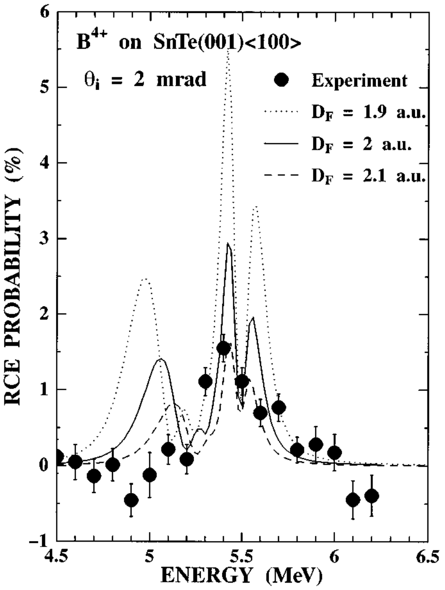

FIG. 7. Comparison between the calculated and observed RCE probabilities. The agreement is reasonably good except for the peak around 5 MeV [corresponding to $(2s+2p_z)$-like state] in the calculated results, which is not seen in the observed result. The absence of the $(2s+2p_z)$-like state might be attributed to the short lifetime of the state near the surface.

bound electron in the $(2s+2p_z)$-like state is localized in the lower side (surface side) of the ion, where the bound electron is subject to frequent collisions with surface atoms. These frequent collisions make the $(2s+2p_z)$-like state unstable and the corresponding RCE peak disappears.

The obtained freezing distance, $D_F \approx 2$ a.u., is slightly smaller than the previous result, $D_F \approx 3$ a.u., for 2-MeV carbon ions [18]. This is consistent with the fact that the charge exchange probability decreases and so D_F decreases with ion energy. This suggests that more pronounced RCE can be observed using ions of higher energy.

IV. CONCLUSIONS

The adiabatic changes of the bound states of the surface channeled B^{4+} ions on the SnTe(001) along the on-string trajectory are calculated taking account of the continuum string potential as well as the induced image potential. Including these adiabatic changes, the RCE probability due to the periodic component of the surface potential is calculated by solving the time-dependent Schrödinger equation along the trajectory. The calculated RCE probability is much larger than the observed result, suggesting that the subsequent charge exchange processes erase almost completely the change in the charge state distribution due to the RCE. Using a freezing distance model for the charge exchange processes at the surface, the RCE probability is calculated. The calculated result agrees well with the observed result except for the disappearance of the excitation to the $(2s+2p_z)$-like state in the observation. The disappearance of the excitation to the $(2s+2p_z)$-like state can be understood by the fact that the $(2s+2p_z)$-like state is unstable near the surface.

ACKNOWLEDGMENTS

We are grateful to the members of the Department of Nuclear Engineering at Kyoto University for the use of the Tandetron accelerator. This work was supported in part by a Grant-in-Aid for Scientific Research from the Ministry of Education, Science, Sports and Culture.

[1] V. V. Okorokov, Pis'ma Zh. Eksp. Teor. Fiz. **2**, 175 (1965) [JETP Lett. **2**, 111 (1965)].

[2] S. Datz, C. D. Moak, O. H. Crawford, H. F. Krause, P. F. Dittner, J. Gomez del Campo, J. A. Biggerstaff, P. D. Miller, P. Hvelplund, and H. Knudsen, Phys. Rev. Lett. **40**, 843 (1978).

[3] C. D. Moak, S. Datz, O. H. Crawford, H. F. Krause, P. F. Dittner, J. Gomez del Campo, J. A. Biggerstaff, P. D. Miller, P. Hvelplund, and H. Knudsen, Phys. Rev. A **19**, 977 (1979).

[4] F. Fujimoto, K. Komaki, A. Ootuka, E. Vilalta, Y. Iwata, Y. Hirota, T. Hasegawa, M. Sekiguchi, A. Mizobuchi, T. Hattori, and K. Kimura, Nucl. Instrum. Methods Phys. Res. B **33**, 354 (1988).

[5] S. Datz, P. F. Dittner, J. Gomez del Campo, K. Kimura, K. F. Krause, T. M. Rosseel, C. R. Vane, Y. Iwata, K. Komaki, Y. Yamazaki, F. Fujimoto, and Y. Honda, Radiat. Eff. Defects Solids **117**, 73 (1991).

[6] K. Kimura, J. P. Gibbons, S. B. Elston, C. Biedermann, R. DeSerio, N. Keller, J. C. Levin, M. Breinig, J. Burgdörfer, and I. A. Sellin, Phys. Rev. Lett. **66**, 25 (1991).

[7] E. Kupfer, H. Gabriel, and J. Burgdörfer, Z. Phys. A **300**, 35 (1981).

[8] J. Burgdörfer, H. Gabriel, and E. Kupfer, Nucl. Instrum. Methods Phys. Res. **194**, 337 (1982).

[9] A. Elci, Phys. Rev. Lett. **53**, 1696 (1984).

[10] R. Kawai and M. Kawai, Surf. Sci. **195**, 535 (1988).

[11] F. J. Garcia de Abajo, V. H. Ponce, and P. M. Echenique, Phys. Rev. Lett. **69**, 2364 (1992).

[12] J. Burgdörfer (private communication).

[13] K. Kimura, H. Ida, M. Fritz, and M. Mannami, Phys. Rev. Lett. **76**, 3850 (1996).

[14] K. Kimura, H. Ida, M. Fritz, and M. Mannami, in *Application of Accelerators in Research and Industry*, edited by J. L. Duggan and I. L. Morgan (AIP, New York, 1997), p. 149.

[15] Y. Fujii, K. Kishine, K. Narumi, K. Kimura, and M. Mannami, Phys. Rev. A **47**, 2047 (1993).

[16] O. H. Crawford and R. H. Ritchie, Phys. Rev. A **20**, 1848 (1979).

[17] Y. H. Ohtsuki, *Charge Beam Interaction with Solids* (Taylor & Francis, London, 1983), p. 230.

[18] M. Fritz, K. Kimura, H. Kuroda, and M. Mannami, Phys. Rev. A **54**, 3139 (1996).